



# Esterification of used cooking oil using ZSM-5 and HY zeolite catalysts for low-cost biodiesel feed production

Teguh Riyanto <sup>ab\*</sup> , Hermawan Dwi Ariyanto <sup>a</sup>, Anggun Puspitarini Siswanto <sup>a</sup>

**a:** Industrial Chemical Engineering Technology, Vocational College, Universitas Diponegoro , Semarang 50275, Indonesia

**b:** Laboratory of Plasma-Catalysis (R3.5), Center of Research and Services - Diponegoro University (CORES-DU), Universitas Diponegoro , Semarang 50275, Indonesia

\* Corresponding author: [teguh\\_ryt@live.undip.ac.id](mailto:teguh_ryt@live.undip.ac.id)

## Abstract

The increasing demand for biodiesel has prompted the investigation of low-quality feedstocks, such as used cooking oil (UCO), as an alternative to refined vegetable oils. Nevertheless, the high free fatty acid (FFA) content, typically indicated by the acid value, in these feedstocks poses challenges in the conventional biodiesel production process using homogeneous alkaline catalysts. This study investigates the use of zeolite-based catalysts, ZSM-5 and HY, for the esterification of UCO to produce biodiesel feed. The catalysts were analyzed through techniques such as X-ray Diffraction (XRD), Brunauer-Emmett-Teller - Barrett-Joyner-Halenda (BET-BJH), and NH<sub>3</sub>-probed temperature-programmed desorption (NH<sub>3</sub>-TPD). XRD analysis revealed distinct crystal structures for the catalysts, with ZSM-5 exhibiting an orthorhombic MFI structure and HY displaying a cubic Faujasite structure. N<sub>2</sub> physisorption analysis showed the presence of micropores and narrow mesopores in the catalysts, with HY exhibiting a peak at 2.5-5 nm pore sizes and a shoulder at 5-10 nm. NH<sub>3</sub>-TPD analysis indicated that all catalysts possess weak, moderate, and strong acid sites, with ZSM-5 having a higher acid density compared to HY. The effects of catalyst type, molar ratio, catalyst dosage, and reaction temperature on the esterification process were systematically studied. ZSM-5 demonstrated superior performance with a 61.07% FFA conversion rate, while HY achieved a slightly lower conversion rate of 57.64%. This study highlights the potential of zeolite-based catalysts in the sustainable production of biodiesel from low-grade feedstocks, contributing to the development of cost-effective and environmentally friendly processes.

## Key findings

- ZSM-5 and HY zeolite catalysts were comprehensively investigated for used cooking oil (UCO) esterification.
- ZSM-5 had higher acid density and Brønsted acid sites compared to HY.
- Reaction parameters like molar ratio, catalyst dosage, and temperature were investigated.
- ZSM-5 demonstrated superior performance with 61.07% FFA conversion compared to HY.

© 2025, the Authors. This article is published in open access under the terms and conditions of the Creative Commons Attribution (CC BY) license (<http://creativecommons.org/licenses/by/4.0/>), which permits unrestricted reuse of the work in any medium provided the original work is properly cited.

## Accompanying information

### Article history

Received: 25.09.25

Revised: 18.01.26

Accepted: 19.01.26

Available online: 05.02.26

### Keywords

zeolite; esterification; used cooking oil; free fatty acids (FFA); biodiesel; fatty acid methyl ester (FAME)

### Funding

This research was financially supported by Lembaga Penelitian dan Pengabdian Kepada Masyarakat (LPPM) Universitas Diponegoro, Indonesia through the research grant of Riset Dosen Muda (RDM) 2025 (grant no. 222-215/UN7.D2/PP/IV/2025).

### Supplementary information

Transparent peer review: 

### Sustainable Development Goals



## 1. Introduction

The increasing large-scale production of biodiesel globally has resulted in an increased demand to develop more innovative, cost-effective, and efficient processes. Increasingly, vegetable oils have been used as feedstocks to produce high quality biodiesel [1]. In recent studies, low-grade feedstocks, which have a higher acid value than refined vegetable oils due to their free fatty acid (FFA) content, are being extensively researched as alternatives to vegetable oils in biodiesel production [2]. When the FFA content in the feedstock surpasses 0.5% of the oil's weight, employing homogeneous alkaline technology with sodium hydroxide as a catalyst is not advisable because it can lead to soap formation and deplete the catalyst [3]. High FFA content in the feedstock leads to soap formation, decreased biodiesel yield, increased production costs, and will make it more difficult to separate and purify the biodiesel product [4–6]. To overcome these problems, esterification is used to reduce FFA in low-grade feedstocks, such as used cooking oil (UCO).

Esterification plays an essential role in the biodiesel production process, where FFAs are transformed into fatty acid methyl esters (FAME) through the use of homogeneous acid catalysts. Typically, this process involves a reaction between FFAs and alcohol, facilitated by an acid catalyst, often sulfuric acid [7]. Homogeneous acid catalysts are known for their effective catalytic performance in the esterification of FFAs. However, the separation of the acid catalyst from the product requires washing with water, which ultimately leads to FAME loss, high energy consumption, and generates a large amount of wastewater [3]. Moreover, homogeneous acid catalysts lead to reactor corrosion and are challenging to regenerate, which raises the overall cost of the production of biodiesel [3,8]. These issues associated with homogeneous catalysts can be addressed by employing heterogeneous catalysts. Not only do they minimize corrosion, but they can also be easily separated and reused without diminishing their quantity or effectiveness [9]. In addition, the use of heterogeneous catalysts can minimize the number of operating units because heterogeneous catalysts can be separated easily from reaction products [10]. Therefore, the use of heterogeneous catalysts is suggested to be more economical.

The ideal heterogeneous acid catalyst for use in esterification reactions should have many strong acid sites, be inexpensive, and exhibit good stability. The selection of an appropriate heterogeneous acid catalyst can simplify product separation and reduce waste formation [11]. In addition, heterogeneous acid catalysts possess higher thermal stability and catalytic activity compared to base catalysts. Due to these specific abilities, heterogeneous acid catalysts are widely used in esterification reactions when the raw materials contain high levels of FFA. Some heterogeneous acid catalysts that have already been developed for use in the esterification process include heteropoly acids [12], zeolites

[13], sulfated metal oxides [14], ordered mesoporous carbon (OMC) [10], and ion exchange resins [15,16].

Zeolite-based catalysts are increasingly recognized for their efficacy in the esterification and transesterification of UCO for biodiesel production. The use of zeolite-supported systems, especially those modified with metal oxides, shows promising results in enhancing the catalytic activity due to their structural and surface properties. One of the notable studies involves the use of a  $\beta$ -zeolite-supported sulfate metal oxide catalyst system. This system includes pure  $\beta$ -zeolite, ZnO- $\beta$ -zeolite, and  $\text{SO}_4^{2-}$ /ZnO- $\beta$ -zeolite variants for biodiesel production using WCO. Among these, the  $\text{SO}_4^{2-}$ /ZnO- $\beta$ -zeolite catalyst demonstrated superior performance, largely attributed to its large pore size and high acidity, which facilitate the conversion of UCO to biodiesel through simultaneous transesterification and esterification. The catalyst achieved a conversion rate of 96.9% under optimal conditions, which include a 3.0 wt.% catalyst loading, 200 °C reaction temperature, and a 15:1 methanol-to-oil molar ratio over an 8 h reaction period [17].

The stability and reusability of such catalysts are crucial for sustainable industrial applications. The  $\text{SO}_4^{2-}$ /ZnO- $\beta$ -zeolite catalyst, for instance, maintained a biodiesel conversion rate of over 80% after three synthesis cycles, highlighting its robustness and potential for repeated use [17]. In addition to the  $\beta$ -zeolite catalyst, other types include the phosphotungstic-based Wells-Dawson compounds. These have also been effective for the transesterification of UCO. For example, the phosphotungstic Wells-Dawson heteropolyacid dispersed on titania oxide showed a conversion rate of 74.6% of glycerides and a yield of 74.4% towards fatty acid methyl esters under specified conditions [18]. Zeolites provide several advantages in catalytic processes. Their large surface area, high acidity, and structural integrity under reaction conditions make them suitable candidates for use with low-cost feedstocks like UCO, which often contain high levels of free fatty acids (FFAs). This feature of being insensitive to FFAs allows them to achieve high biodiesel yields even when traditional homogeneous catalysts might fail due to soap formation and other issues [17].

Although many researchers have reported on many types of suitable heterogeneous catalysts for FFA esterification, to the best of our knowledge, the specific studies on the comparison of zeolite type are limited. Therefore, this work investigates the catalytic performance of two zeolite-based solid acid catalysts, mainly ZSM-5 and HY, in the esterification of UCO with methanol. The research aims to elucidate the relationship between the physicochemical properties of these zeolite catalysts and their catalytic activity in UCO esterification. A comprehensive characterization of the ZSM-5 and HY catalysts was conducted to analyze their crystal structure, textural properties, and surface acidity. X-ray diffraction (XRD), nitrogen physisorption, and temperature-programmed desorption of ammonia ( $\text{NH}_3$ -TPD) techniques were employed to probe the catalysts' structural and

acidic characteristics. Additionally, the catalytic performance of ZSM-5 and HY was evaluated under various reaction conditions, including different catalyst dosages, methanol-to-oil ratios, and reaction temperatures. By correlating the catalysts' properties with their esterification activity, this study seeks to provide insights into the key factors influencing FFA conversion in UCO. The findings are expected to contribute to the development of more efficient solid acid catalysts for biodiesel production from low-quality feedstocks like UCO. Furthermore, the optimization of reaction parameters investigated here can inform process design considerations for the industrial-scale implementation of UCO esterification using zeolite catalysts.

## 2. Materials and Methods

### 2.1. Materials

The used cooking oil (UCO) that was used in this study was obtained from a local fast food restaurant. The acid value of the UCO was determined to be  $8.47 \pm 0.043$  mg KOH/g. Table 1 shows the properties of the UCO that was used in this study. Methanol (99.9%) was obtained from Merck. The ZSM-5 (CBV8014) and HY (CBV760) zeolites were obtained from Zeolyst.

### 2.2. Catalyst characterization methods

The catalysts underwent comprehensive characterization using a combination of analytical techniques to elucidate their structural, textural, and surface properties. X-ray Diffraction (XRD) method was used to investigate the presence of the crystalline phases in the catalysts. The analysis was conducted using Cu K $\alpha$  radiation. The diffraction patterns were collected with a scanning speed of  $4^\circ \text{ min}^{-1}$  in  $2\theta$  angle ranges of  $5^\circ$  to  $90^\circ$  [19]. The Brunauer-Emmet-Teller (BET) method was used to determine catalyst surface area of the catalysts, while the Barret-Joyner-Halenda (BJH) method was used to determine the pore size distribution [19]. In order to determine the catalysts' acidity strengths,  $\text{NH}_3$ -probed Temperature Programmed Desorption ( $\text{NH}_3$ -TPD) was utilized. The adsorption of the probe component was conducted at  $100^\circ \text{ C}$ , and then the desorption was conducted from  $100^\circ \text{ C}$  to  $900^\circ \text{ C}$  with a heating rate of  $10^\circ \text{ C/min}$  [20]. Furthermore, the Brønsted and Lewis acid sites on the catalysts were analysed using Pyridine-probed FT-IR [19].

### 2.3. Esterification process

The esterification of FFA in UCO was conducted in a 100 mL round bottom flask fitted with a reflux condenser (Figure 1). In the flask, 20 g of UCO and methanol were mixed. Subsequently, a catalyst was introduced to the mixture, which was then stirred using a magnetic stirrer. In this study, the stirring speed was set to be constant at 300 rpm. Unless specified otherwise, the reaction temperature was kept at  $50^\circ \text{ C}$  with the help of a heating mantle. The study examined

the influence of the methanol to UCO molar ratio (ranging from 5:1 to 20:1), catalysts dosage (0.025 to 0.15 g/g-UCO), reaction temperature ( $40$ – $65^\circ \text{ C}$ ), and reaction time (0–2 h). The range of reaction conditions was adopted and varied based on several sources in the literature [21,22]. Specifically, to investigate the effect of catalysts type, the experiment was conducted using a methanol to UCO ratio of 10, a temperature of  $50^\circ \text{ C}$ , and a catalyst dosage of 0.075 g/g-UCO with varied reaction time (between 15 min and 120 min), and for each time variable a fresh batch of 20 g of used cooking oil (UCO) was used. The reaction was terminated at the specified time before sampling. The effect of methanol to UCO molar ratio on FFA conversion was examined at a temperature of  $50^\circ \text{ C}$  and a catalyst dosage of 0.05 g/g-UCO. The effect of catalyst dosage on FFA conversion was examined at a reaction temperature of  $50^\circ \text{ C}$  and a methanol to UCO molar ratio of 10. The effect of reaction temperature on FFA conversion was examined at a catalyst dosage of 0.05 g/g-UCO and a methanol to UCO molar ratio of 10. The resulting reaction mixture was centrifuged, and the oil phase was subsequently analysed.

### 2.4. Product analysis

The calculation of the acid value takes into account the volume of potassium hydroxide used in the titration, its normality, and the weight of the sample.

**Table 1** Properties of UCO used in this study.

| Parameter   | Value              |
|---|--------------------|
| Density at $20^\circ \text{ C}$ (g/mL)            | $0.904 \pm 0.0003$ |
| Kinematic viscosity at $20^\circ \text{ C}$ (cSt) | $76.91 \pm 1.75$   |
| Moisture content (wt.%)                           | $0.319 \pm 0.001$  |
| Acid value (mg KOH/g)                             | $8.47 \pm 0.043$   |

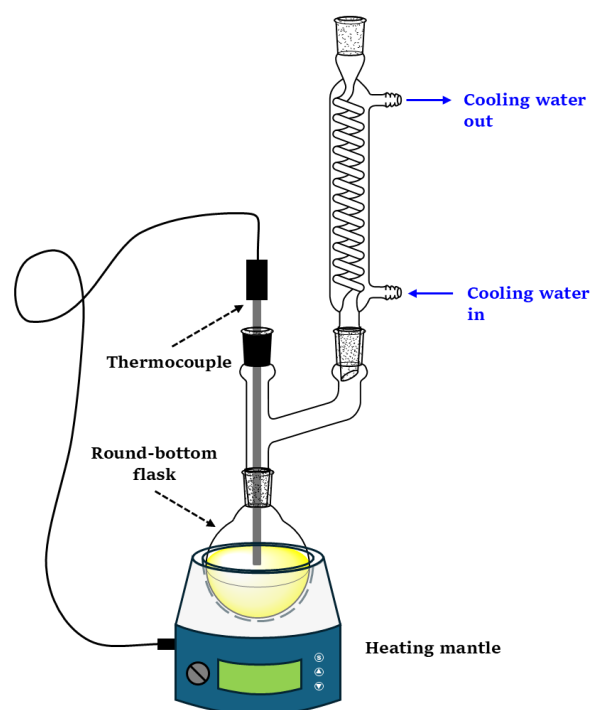


**Figure 1** Experimental set up.

This value represents the number of milligrams of potassium hydroxide required to neutralize the free fatty acids present in one gram of the sample. The acid value was calculated using Equation (1) [23].

$$AV = \frac{(V_t - V_o) \cdot M \cdot 56.1}{m}, \quad (1)$$

where AV represents the acid value measured in mg KOH per gram of oil,  $V_t$  denotes the volume of the titrant solution used for the sample titration, measured in mL, while  $V_o$  indicates the volume of the titrant solution used for the blank titration, also in mL.  $M$  stands for the molarity of the titrant solution, expressed in mol/L, and  $m$  refers to the mass of the sample in g. The acid value analysis for each sample was performed in duplicate, and the reported values represent the average of two independent measurements.

The conversion of FFA was calculated based on acid value in the UCO using Equation (2) which was adopted from literature [24,25]:

$$\text{FFA conversion (\%)} = \left( \frac{AV_o - AV_t}{AV_o} \right) \cdot 100, \quad (2)$$

where  $AV_o$  stands for the acid value in UCO before esterification and  $AV_t$  stands for the acid value in UCO after esterification.

### 3. Results and Discussions

#### 3.1. Catalyst characteristics

##### 3.1.1. Crystal structure and surface functional group of the catalysts

The XRD analysis revealed distinct crystal structures for the ZSM-5 and HY catalysts. Figure 2 shows the XRD patterns and FT-IR spectra of HY and ZSM-5 catalysts. As shown in Figure 2, the ZSM-5 catalyst exhibited an orthorhombic MFI structure, characterized by intense peaks at specific  $2\theta$  angles corresponding to various crystallographic planes. Notably, a characteristic quintet of the MFI structure was observed at  $2\theta = 23\text{--}25.5^\circ$ , consistent with findings from previous studies by Zang et al. [26] and Riyanto et al. [27]. This structural identification was based on the Crystallography Open Database (COD) reference code 96-154-0268, attributed to the presence of prominent peaks at  $2\theta = 7.95^\circ$ ,  $8.89^\circ$ ,  $23.49^\circ$ ,  $23.71^\circ$ ,  $24.13^\circ$ ,  $24.35^\circ$ , and  $24.83^\circ$ , which correspond to the (101), (020), (501), (051), (151), (303), and (133) planes, respectively. In contrast, the HY-based catalysts displayed a cubic Faujasite (FAU) structure, evidenced by diffraction peaks at  $2\theta = 6.52^\circ$ ,  $10.54^\circ$ ,  $12.32^\circ$ ,  $16.14^\circ$ ,  $19.22^\circ$ ,  $20.93^\circ$ ,  $24.27^\circ$ ,  $27.72^\circ$ , and  $32.15^\circ$ . These peaks correspond to (111), (220), (311), (331), (511), (440), (533), (642), and (555) planes, as confirmed by the COD reference code 96-153-6102. The observed FAU structure aligns with previous research conducted by Reinoso et al. [28].

The distinct diffraction patterns of ZSM-5 and HY catalysts highlight their unique crystal structures, which are crucial for understanding their catalytic properties and potential applications in various chemical processes. Moreover, the intensity and sharpness of the diffraction peaks for both ZSM-5 and HY catalysts indicate high crystallinity and well-defined structures. These structural characteristics play a significant role in determining the catalytic activity and selectivity of the zeolites. The presence of specific crystallographic planes and their corresponding intensities can provide insights into the distribution of active sites and pore accessibility, which are crucial factors in catalyst performance. Therefore, further characterisations should be conducted to elucidate the relationship between crystallographic planes and catalytic properties for WCO esterification, such as surface acid properties and pore size distribution.

The broad absorption bands observed between  $3750$  and  $3400\text{ cm}^{-1}$  are attributed to the stretching vibrations of the OH groups in water molecules, while the band around  $1630\text{ cm}^{-1}$  corresponds to the bending vibration mode of residual  $\text{H}_2\text{O}$  molecules [29]. The absorption band at  $1225\text{ cm}^{-1}$  in ZSM-5 and  $1204\text{ cm}^{-1}$  in HY is likely due to the external vibrations between  $\text{SiO}_4$  and  $\text{AlO}_4$  tetrahedra of the zeolite [29,30]. The band at  $1175\text{ cm}^{-1}$  in HY and at  $1103\text{ cm}^{-1}$  in ZSM-5 represents the asymmetric stretching of Si-O-Si or Si-O-Al bonds [31]. The band at  $833\text{ cm}^{-1}$  is indicative of the Si-O, SiO-Al, and Al-OH stretching vibrations associated with the internal  $\text{TO}_4$  structure (T = Si, Al). The band around  $790\text{ cm}^{-1}$  corresponds to the symmetrical stretching vibrations of the external  $\text{TO}_4$  structure [29,30]. Additionally, the band detected around  $455\text{ cm}^{-1}$  is attributed to the internal vibrations of TO (tetrahedrons) and around  $550\text{ cm}^{-1}$  is attributed to the vibrations of the secondary building units [31].

##### 3.1.2. Textural properties of catalysts

The efficiency of a catalytic reaction significantly depends on the diffusion of reactants to the active sites within the catalyst pores and subsequent product diffusion away from the sites. Therefore, it is important to analyse the catalysts' pore structure. The  $\text{N}_2$  physisorption analysis of HY and ZSM-5 catalysts provides valuable insights into their pore structures, revealing a complex network of micropores and potential narrow mesopores. As can be seen in Figure 3(A), the catalysts show a sharp adsorption at low relative pressures ( $p/p^\circ < 0.01$ ) which is a clear indicator of narrow micropores in all catalysts, as noted by Thommes et al. [32]. This characteristic suggests that the catalysts possess a diverse range of pore sizes, extending beyond just narrow micropores to include wider micropores and possibly narrow mesopores around  $2.5\text{ nm}$  in diameter. Such a varied pore size distribution can significantly impact the catalysts' performance, affecting their adsorption capacity, selectivity, and overall catalytic activity.

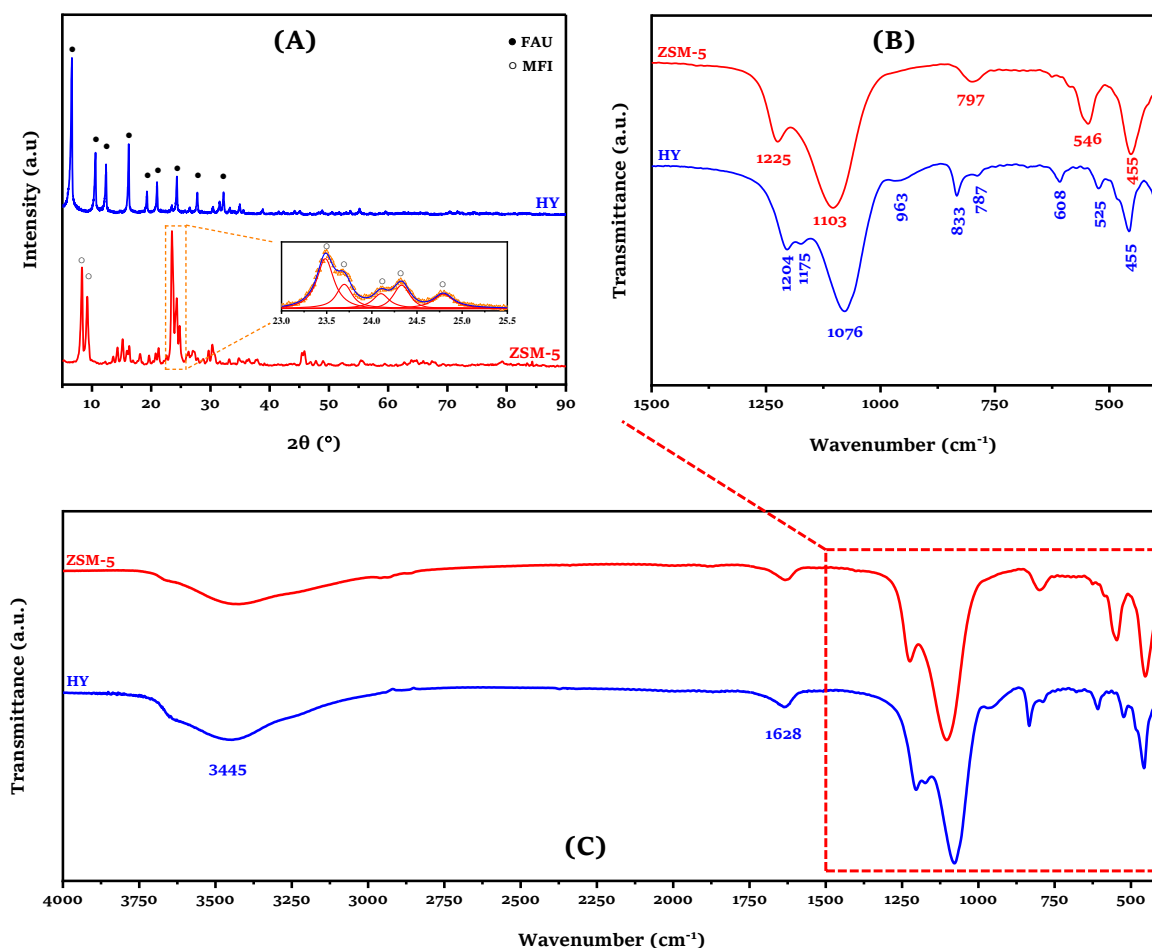


Figure 2 XRD patterns and FT-IR spectra of HY and ZSM-5 catalysts.

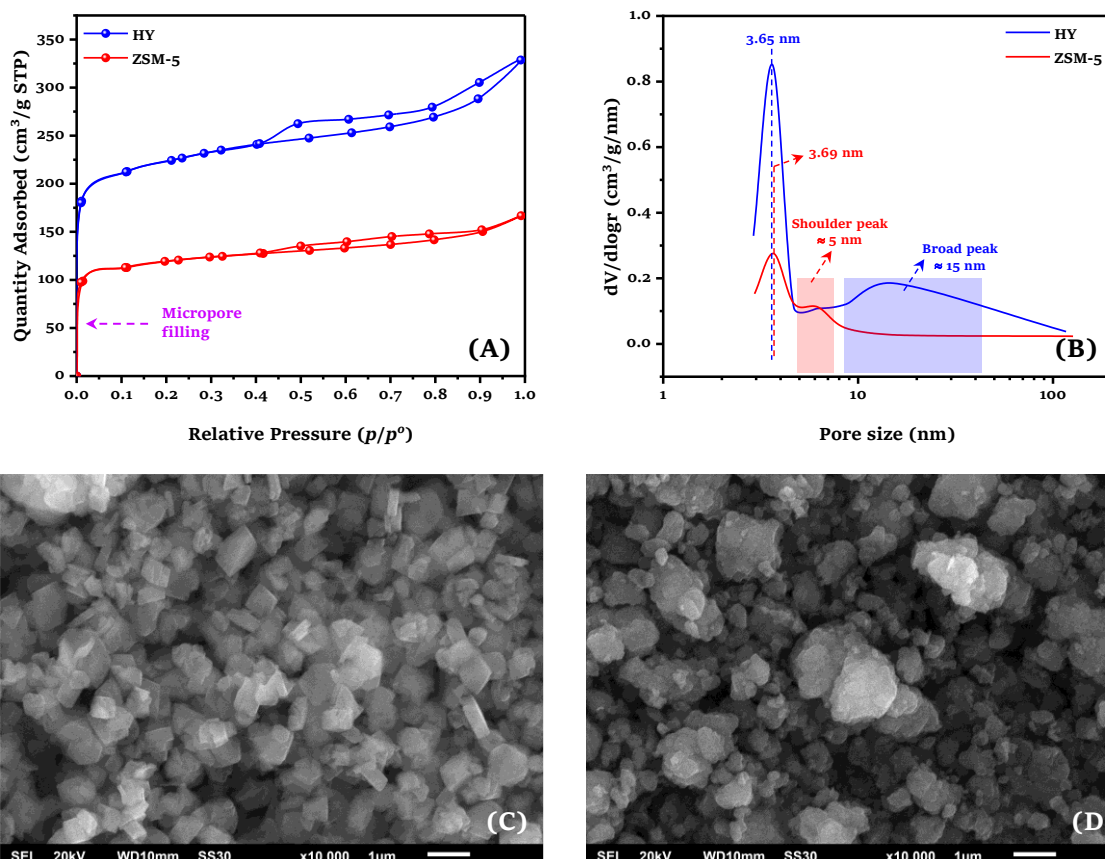


Figure 3 (A) N<sub>2</sub> sorption isotherms, (B) catalysts pore size distribution, and SEM analysis analysis of (C) HY and (D) ZSM-5 zeolites.

Furthermore, the presence of a hysteresis loop in the  $N_2$  sorption isotherms further classifies these catalysts under Type H4 according to the IUPAC classification system. This classification not only confirms the existence of micropores, but also provides additional information about the nature of the pore network. Type H4 hysteresis is often associated with narrow slit-like pores or the internal voids of loose assemblages of plate-like particles [33]. This pore structure can have important implications for the catalysts' behavior in various applications, such as their ability to facilitate mass transfer of reactants and products, their resistance to deactivation through coking, and their potential for shape-selective catalysis. The combination of micropores and narrow mesopores in these catalysts can create a hierarchical pore structure, which is often desirable for optimizing catalytic performance in complex reactions.

The physisorption isotherms of the catalysts reveal a complex pore structure that combines characteristics of both Type I and Type II adsorption. This hybrid behavior, observed at  $p/p^0 = 0.4$ , indicates the simultaneous presence of micropores and narrow mesopores within the catalyst materials. The coexistence of these two pore types creates a hierarchical pore structure that can significantly influence the catalytic performance. Notably, the HY and ZSM-5 catalysts exhibit a particularly intricate pore architecture, with a distinct peak in the pore size distribution at 2.5–5 nm and a shoulder extending to 5–10 nm, as shown in Figure 3(B). This bimodal distribution suggests a well-developed mesoporous network complementing the inherent microporous structure of the zeolite framework. The dual pore structure observed in these catalysts has important implications for their catalytic applications. Micropores, typically less than 2 nm in diameter, provide high surface area and shape selectivity, which are crucial for molecular sieving and selective catalysis. On the other hand, mesopores, ranging from 2 to 50 nm, facilitate the diffusion of larger molecules and enhance mass transfer within the catalyst. The combination of these pore types can lead to synergistic effects, where the micropores offer active sites for catalysis while the mesopores improve accessibility and reduce diffusion limitations. Moreover, as can be seen in Table 2, both HY and ZSM-5 catalysts have a high surface area. The surface areas of HY and ZSM-5 catalysts are 700  $m^2/g$  and 370  $m^2/g$ , respectively. In addition, the total pore volumes of HY and ZSM-5 catalysts are 0.51  $m^3/g$  and 0.26  $m^3/g$ , respectively. It suggested that these catalysts provide more effective mass transfer. Klawekla et al. [34] reported that

high surface area catalysts can reduce mass transfer barriers by providing more pathways for reactants to reach the catalytic sites, thus enhancing reaction rates. These characteristics making HY and ZSM-5 catalysts suitable for wide range of applications, especially for WCO esterification. The diffusion limitation of FFA molecules can be reduced, since these catalysts have mesopores structure.

The SEM analysis revealed distinct surface morphologies for the HY and ZSM-5 catalysts, providing valuable insights into their structural characteristics. As can be observed in Figure 3(C), the HY catalyst exhibited smooth agglomerate particles with irregular polyhedral morphology, a typical characteristic of the cubic FAU structure. This observation aligns with previous studies that have reported similar morphological features for FAU zeolites, including irregular polyhedral [35] and octahedral [36] structures. The smooth surface and well-defined polyhedral shapes of the HY catalyst particles indicate a high degree of crystallinity and structural uniformity.

In contrast, the ZSM-5 catalyst displayed a rough and irregular surface morphology (Figure 3(D)), attributable to its corresponding MFI structure. This distinct surface characteristic of ZSM-5 is a result of its unique framework topology, consisting of intersecting straight and sinusoidal channels. The rough surface morphology of ZSM-5 can contribute to enhanced accessibility of active sites, potentially improving its catalytic activity. The observed differences in surface morphology between HY and ZSM-5 catalysts highlight the importance of zeolite structure in determining their physical properties and, consequently, their catalytic behavior.

### 3.1.3. Catalysts acidic properties

The role of catalyst acidity is crucial in the esterification process. Roslan et al. [37] reported that the optimal heterogeneous acid catalyst for esterification should possess a large number of strong acid sites. Therefore, the surface acidic properties of the catalysts should be evaluated. The  $NH_3$ -TPD (Temperature-Programmed Desorption of Ammonia) analysis provides valuable insights into the acid site properties of HY and ZSM-5 catalysts, offering a comprehensive understanding of their catalytic behavior. In this study, the adsorption of ammonia onto catalysts surface was conducted at 100 °C. This temperature is carefully chosen to ensure that the observed interactions are primarily due to chemical adsorption on the catalysts' acid sites, rather than physical adsorption. This approach allows for an accurate assessment of total acidity, providing a reliable measure of the catalyst's acid site density and distribution.

**Table 2** Catalyst's pore structure properties.

| Catalysts | $S_{BET}$ ( $m^2/g$ ) | $S_{micro}^*$ ( $m^2/g$ ) | $S_{ext}^*$ ( $m^2/g$ ) | $V_{micro}^*$ ( $cm^3/g$ ) | $V_{total}$ ( $cm^3/g$ ) | $d_p^{\ddagger}$ (nm) | $d_{ave}^{\ddagger}$ (nm) |
|-----------|-----------------------|---------------------------|-------------------------|----------------------------|--------------------------|-----------------------|---------------------------|
| HY        | 700                   | 544                       | 156                     | 0.28                       | 0.51                     | 3.65                  | 2.90                      |
| ZSM-5     | 370                   | 296                       | 74                      | 0.15                       | 0.26                     | 3.69                  | 2.79                      |

\*Based on t-plot method;

†Pore size based on BJH method;

‡Average pore size based on BET method;

The temperature at which ammonia desorbs indicates the acid strength of catalysts. The acid strengths are typically categorized into three distinct ranges: weak (120–300 °C), moderate (300–500 °C), and strong (>500 °C) [38,39]. This classification enables researchers to quickly assess the distribution of acid site strengths within a catalyst sample. Figure 4 illustrates the NH<sub>3</sub>-TPD signals for the HY and ZSM-5 catalysts, while Table 3 provides a summary of the catalysts' acid strength.

As can be observed in Figure 4, all catalysts have three main desorption peaks, which appear at 120–300 °C, 300–500 °C, and >500 °C. This fact confirms that all catalysts have both weak, moderate, and strong acid sites. The parent HY catalyst exhibits a balanced distribution of weak and moderate acid sites, suggesting a more versatile acidity profile suitable for reactions requiring milder acid conditions. In contrast, the ZSM-5 catalyst demonstrates a predominance of moderate and strong acid sites, indicating its potential for catalyzing reactions that demand higher acid strength. According to Chen et al. [40] and Hensen et al. [41], the strong acid site corresponds to the Brønsted acid site, meaning that ZSM-5 catalyst has more Brønsted acid site than HY catalyst. The difference in Brønsted acidity between ZSM-5 and HY catalysts can be attributed to their distinct structural properties. The Brønsted acid sites on the zeolite-based catalyst are the sites that can donate protons (H<sup>+</sup>) (proton donor), while the Lewis acid sites on the zeolite-based catalyst are sites that can accept electron pairs (electron acceptor) [42].

The presence of Brønsted and Lewis acid sites in the zeolite-based catalysts structure is shown in Figure 4(C). The adsorption band for the Lewis acid site is located at a wavenumber of ~1450 cm<sup>-1</sup>, while the Brønsted acid site appears at ~1550 cm<sup>-1</sup> [43]. The quantity of Brønsted and Lewis acid sites on the catalyst can be determined by examining the area of each respective peak. It shows that the peak area for the Brønsted acid site suggests that ZSM-5 possesses a greater number of Brønsted acid sites compared to HY. A similar observation applies to the Lewis acid site. This finding aligns with the NH<sub>3</sub>-TPD analysis. Brønsted acid site consists of a hydrogen atom bonded to the oxygen atom that connects the tetrahedrally coordinated cations, which form the zeolitic framework [42]. The Lewis acid sites in zeolite-based catalysts are electron deficient sites (containing unoccupied orbitals) exhibiting the ability to accept electrons during interactions with molecules which can be formed through the dehydration process in the zeolite framework [42,44]. A higher amount of Brønsted acid site in ZSM-5 catalyst is expected to increase the esterification process of UCO. Furthermore, the total acidity and the acid density of the ZSM-5 catalyst are notably higher than those of HY catalyst. As shown in Table 3, the total acidity of ZSM-5 and HY catalysts are 620 μmol-NH<sub>3</sub>/g-cat and 203 μmol-NH<sub>3</sub>/g-cat, respectively. In addition, the acid density of ZSM-5 (1.58 μmol/m<sup>2</sup>) is approximately eight times higher than

that of the HY catalyst (0.27 μmol/m<sup>2</sup>). This substantial difference in acid site concentration and strength distribution between the two catalysts implies distinct catalytic performances and selectivities in acid-catalyzed reactions.

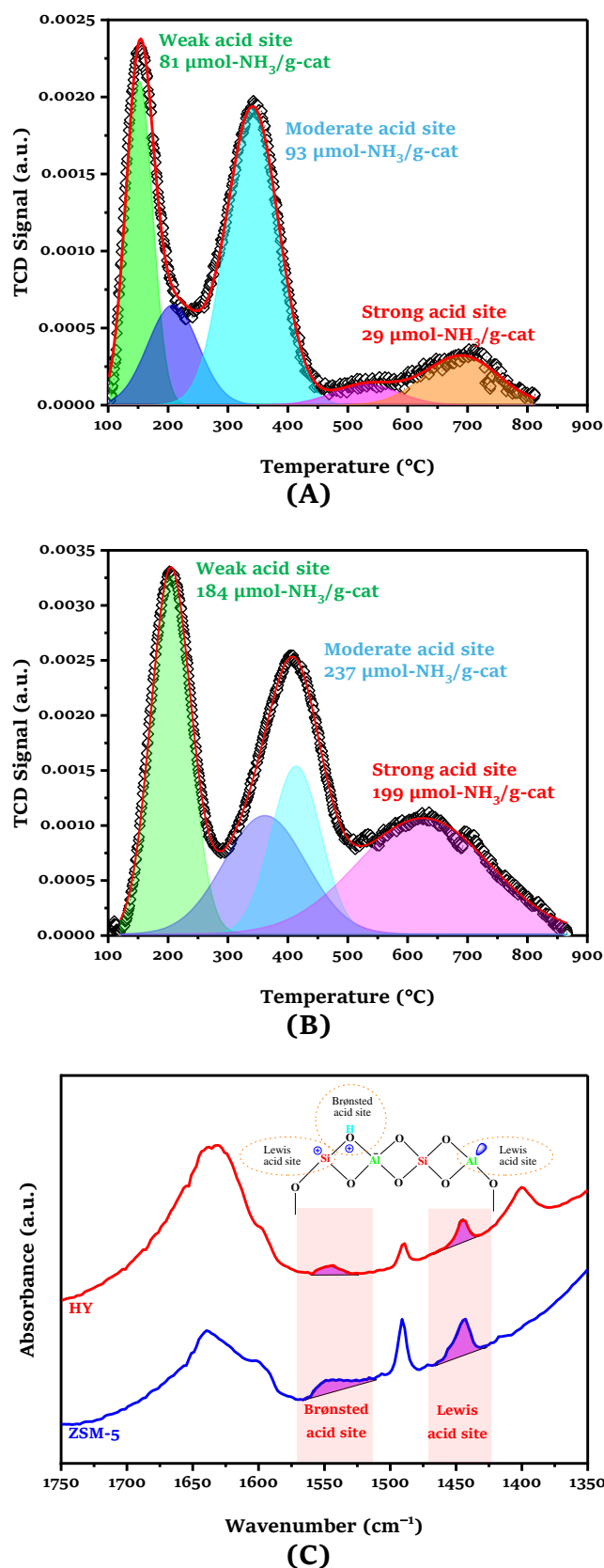


**Figure 4** TPD signal of (A) HY catalyst and (B) ZSM-5 catalyst and (C) the Pyridine-probed FT-IR of HY and ZSM-5 catalysts.

**Table 3** Catalysts acidity.

| Catalysts | Acid site amount ( $\mu\text{mol-NH}_3/\text{g-cat}$ ) |           |        |       | Acid density <sup>a</sup> ( $\mu\text{mol/m}^2$ ) |
|-----------|--|-----------|--------|-------|---|
|           | Weak   | Mod-erate | Strong | Total |   |
| HY        | 81   | 93        | 29     | 203   | 0.27  |
| ZSM-5     | 184  | 237       | 199    | 620   | 1.58  |

<sup>a</sup>Ratio of total acidity to BET surface area

## 3.2. Esterification

### 3.2.1. The effect of catalysts type

The catalytic performances of the HY and ZSM-5 catalysts in the esterification of UCO with methanol were examined under specific operating conditions. The initial acid value of the UCO was determined to be  $8.47 \pm 0.043$  mg KOH/g, indicating a significant presence of free fatty acids. To investigate the effect of catalysts type, the operating conditions were kept consistent for both catalysts to ensure a fair comparison of their performance. By comparing the catalytic activities of HY and ZSM-5 under identical conditions, this study sought to determine which catalyst would be more efficient in facilitating the esterification reaction, potentially leading to improved biodiesel production processes using used cooking oil as a renewable feedstock.

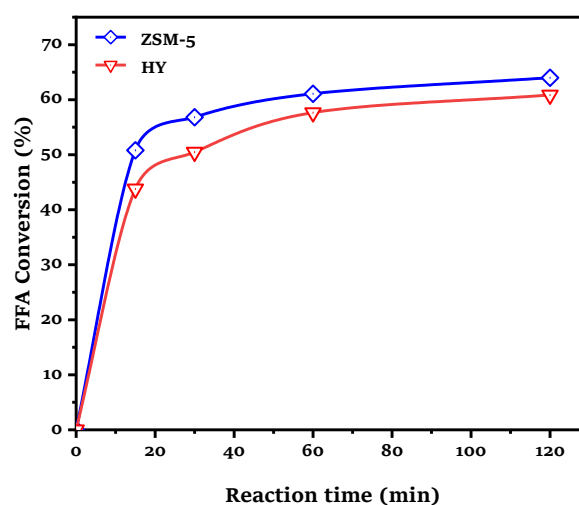
The conversion of FFA using zeolite catalysts demonstrates the effectiveness of these materials in catalytic processes. Figure 5 shows the effect of catalyst type on FFA conversion. As can be observed, ZSM-5, a type of zeolite with a specific three-dimensional pore structure, showed a higher FFA conversion rate of 61.07% compared to the HY zeolite catalyst, which achieved 57.64% conversion. This difference in performance can be attributed to the unique properties of the catalysts, such as pore size, acidity, and surface area. The superior performance of ZSM-5 in FFA conversion may be due to its medium-pore structure and high Si/Al ratio, which can enhance its hydrophobicity and acid strength. These characteristics potentially allow for better interactions with FFA molecules and more efficient catalytic conversions. In addition, high FFA conversion using ZSM-5 is attributed by the high acid density and the presence of Brønsted acid site. Based on  $\text{NH}_3$ -TPD (Figure 4(B)) and Pyridine-probed FT-IR analysis (Figure 4(C)), ZSM-5 has higher acid density and more Brønsted acid site than HY.

A higher performance of ZSM-5 than HY catalyst is attributed to their properties. The medium-pore structure of ZSM-5 may provide an optimal environment for FFA molecules to access active sites within the catalyst, leading to enhanced conversion rates. Additionally, the higher Si/Al ratio of ZSM-5 can contribute to increased hydrophobicity, which may facilitate the adsorption of FFA molecules onto the catalyst surface. The acid strength of the catalyst also plays a crucial role in the conversion process, with stronger acid sites potentially promoting more efficient catalytic reactions. Brønsted acid sites are widely known as the main active centers for catalyzing esterification reactions, in-

cluding those involving FFAs and alcohols. These sites function by protonating the carbonyl group of the acid, which increases the electrophilicity of the carbon and facilitates nucleophilic attack by the alcohol, leading to ester and water formation [45,46]. Lewis acid sites can also catalyze esterification, typically by coordinating with the carbonyl oxygen of the acid to form a reactive complex, which similarly enhances the susceptibility of the carbonyl carbon to nucleophilic attack by the alcohol [46,47]. Many studies report that both Brønsted and Lewis acid sites are responsible for catalyzing the esterification reaction, and their coexistence can lead to enhanced catalytic performance due to possible synergistic effects [46,48].

Based on several literature sources, the strength and density of Brønsted acid sites are critical factors. Stronger Brønsted acid sites, such as those found in zeolites and certain metal-organic frameworks (MOFs), can significantly enhance the esterification rate. For instance, Koo et al. [49] reported that the strong Brønsted acid sites in H-ZSM5 and H-Ferrierite zeolites are responsible for the increased esterification rates and selectivity towards methyl acetate. Similarly, Brønsted acid sites in UiO-66 MOFs, enhanced by sulfur functionalization, showed increased catalytic activity for dehydration reactions, which can be analogous to esterification processes [50]. Wang et al. [51] reported that the esterification mechanism involves the activation of FFAs by Brønsted acid sites, followed by the formation of a tetrahedral intermediate with methanol, leading to the production of fatty acid methyl esters (FAME) and water. The rate-determining step is the combination of the activated FFA with methanol, which is facilitated by the strong acidic environment provided by the Brønsted acid sites [51,52].

Table 4 highlights the comparative catalytic activities of various heterogeneous catalysts employed in the free fatty acid (FFA) esterification process. Notably, the ZSM-5 and HY catalysts examined in this study exhibit considerably lower catalytic performance relative to other catalysts such as HMFI [21] and HY(80) [53].

**Figure 5** The effect of catalyst type on FFA conversion.

This disparity in activity can be attributed to multiple experimental parameters, including reaction time, catalyst loading, reaction temperature, and the molar ratio of methanol to FFA. Each of these factors plays a critical role in influencing the efficiency of the esterification reaction, potentially affecting catalyst surface interactions, active site availability, and overall conversion rates.

Since the FFA conversion using ZSM-5 catalyst is higher than using HY catalyst, the effect of methanol to UCO molar ratio, the effect of catalyst dosage, and the effect of reaction temperature were further examined using ZSM-5 catalyst.

### 3.2.2. The effect of methanol to UCO molar ratio

The molar ratio of alcohol to FFA is a critical parameter in the esterification process, influencing not only the conversion efficiency but also the economic viability of the production. While the stoichiometric requirement dictates a 1:1 molar ratio, industrial applications typically employ an excess of alcohol to optimize the reaction outcomes. This surplus alcohol serves multiple purposes: it accelerates the reaction rate, shifts the equilibrium towards product formation, and compensates for any potential side reactions or impurities that may consume alcohol molecules [54,55]. However, determining the ideal alcohol-to-FFA ratio involves a delicate balance between maximizing conversion and minimizing costs. While a higher ratio can lead to improved yields and faster reaction times, it also increases raw material costs and necessitates more extensive downstream separation processes to recover the excess alcohol. Furthermore, an excessively high alcohol concentration may dilute the reaction mixture, potentially reducing the reaction rate and requiring larger reactor volumes. There-

fore, researchers and process engineers must carefully optimize this parameter, considering both the technical benefits and economic implications.

Figure 6 illustrates how the molar ratio of methanol to UCO affects FFA conversion. At first, the FFA conversion rate increased quickly, but then it slowed down. This indicates that the relationship between the methanol-to-oil ratio and FFA conversion is not linear. The FFA conversion significantly increases at methanol-to-oil ratio of 5 to 15. This increase in FFA conversion with the increase in methanol-to-oil ratio is expected. It is well known that the esterification process is reversible. An excess of methanol is essential in shifting the equilibrium.

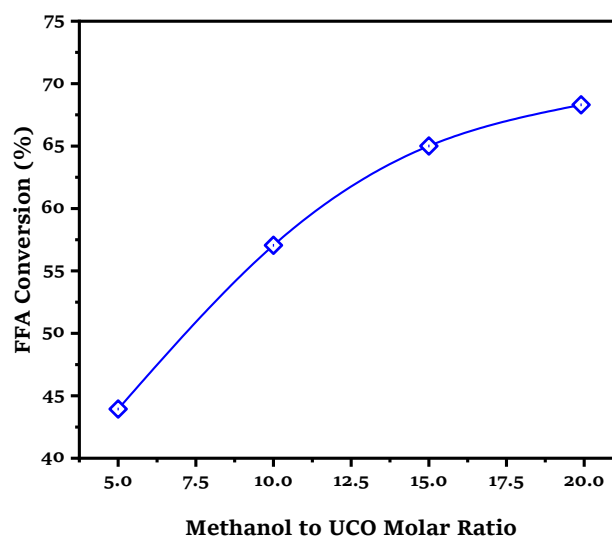


Figure 6 The effect of methanol to UCO molar ratio on FFA conversion.

Table 4 Performance comparison with previous studies.

| Catalyst        | Reaction Condition  | FFA Conversion (%) | Ref.                  |
|-----------------|---|--------------------|-----------------------|
| HMFI            | Reaction temperature = 60 °C.<br>Catalyst amount = 1.0 g.<br>Reaction time = 3 h.<br>Methanol-to-oil molar ratio = 30:1         | 80                 | Chung et al. [21]     |
| H-Y(80) zeolite | Reaction temperature = 68 °C.<br>Catalyst amount = 5 wt.%.<br>Reaction time = 6 h.<br>Methanol to FFA molar ratio = 9:1         | 93.7               | Dal Pozzo et al. [53] |
| SBA-15          | Reaction temperature = 68 °C.<br>Catalyst amount = 7 wt.%.<br>Reaction time = 5 h.<br>Methanol to FFA molar ratio = 15:1        | 50.7               | Xie et al. [56]       |
| Amberlyst-15    | Reaction temperature = 65 °C.<br>Catalyst amount = 4 wt.%.<br>Reaction time = 1.5 h.<br>Methanol-to-oil molar ratio = 15:1      | 60.2               | Gan et al. [57]       |
| ZSM-5           | Reaction temperature = 50 °C.<br>Catalyst amount = 0.075 g/g-UCO.<br>Reaction time = 1 h.<br>Methanol-to-oil molar ratio = 10:1 | 61.07              | This study            |
| HY              | Reaction temperature = 50 °C.<br>Catalyst amount = 0.075 g/g-UCO.<br>Reaction time = 1 h.<br>Methanol-to-oil molar ratio = 10:1 | 57.64              | This study            |

By increasing the molar ratio of methanol to UCO, the reaction is driven towards producing methyl esters and water, thereby effectively lowering the FFA content. This concept, known as Le Chatelier's principle, suggests that when a system at equilibrium is disturbed, it will adjust to counteract the disturbance and establish a new equilibrium. Moreover, from the perspective of mass transfer, increasing the molar ratio of methanol-to-oil reduces the viscosity of the reaction mixture. This reduction facilitates improved interaction between the reactants and the catalyst, thereby boosting the mass transfer rate and ultimately leading to a higher conversion rate within a set reaction period.

As can be observed in Figure 6, the FFA conversion turns to be slower when the methanol to UCO ratio was increased to 20. As shown in Figure 6, it is evident that the lower methanol to UCO ratio was not sufficient for the conversion to reach more than 45%. At methanol-to-oil ratio of 15, 65% conversion was reached after 60 min of reaction. After the methanol to UCO ratio increased to 20, the conversion reached 68%. It indicates that increasing the methanol to UCO ratio beyond 15 does not significantly improve the FFA conversion. This phenomenon is caused by mass transfer limitations and inhomogeneity of reactants. For instance, Yunus et al. [58] reported that increasing the ratio from 6:1 to 12:1 in a semi-batch esterification process led to decreased FFA conversion. Gan et al. [57] observed that the conversion of FFA was initially fast, but as the reaction continued, the formation of water tended to promote the hydrolysis of FAME back into FFA, leading to a reduction in the rate of FFA conversion. A similar result was also reported by Ramadhas et al. [55]: no notable enhancement in FFA conversion was observed with the excessive use of alcohol.

### 3.2.3. The effect of catalyst dosage

The dosage of catalysts in esterification reactions is a critical factor that significantly influences the overall process efficiency and product yield. Higher catalyst concentrations generally lead to increased reaction rates and higher conversions, as they provide more active sites for the reactants to interact. However, there is often an optimal catalyst dosage beyond which further increases may not result in substantial improvements or may even have detrimental effects. Figure 7 illustrates the effect of catalyst dosage on FFA conversion.

Based on Figure 7, the conversion of FFA in UCO is significantly influenced by catalyst dosage. As observed, increasing the catalyst dosage from 0.025 to 0.15 g/g-UCO results in a corresponding increase in FFA conversion. At the lowest dosage of 0.025 g/g-UCO, the conversion rate is 55.31%, which rises to 57.05% when the dosage is doubled to 0.05 g/g-UCO. The highest conversion rate of 62.78% is achieved at the maximum catalyst dosage of 0.1 g/g-UCO. This trend suggests a positive correlation between catalyst

dosage and FFA conversion efficiency. The increase in conversion rate is likely due to the greater availability of active sites for the esterification reaction as more catalysts are introduced. Roslan et al. [37] reported that the increase in catalyst loading leads to a proportional rise in the number of active sites available for the reaction. These active sites serve as crucial points where the reactants can interact with the catalyst, facilitating the conversion process. As more catalyst is introduced into the system, the surface area for potential reactions expands, providing more opportunities for the FFA to come into contact with the catalyst particles. This enhanced availability of active sites significantly improves the mass transfer efficiency between the reactants and the catalyst. The increased contact rate allows for more frequent and effective collisions between FFA molecules and catalyst particles, accelerating the overall reaction kinetics. Consequently, this leads to a higher FFA conversion rate and an overall increase in the reaction rate. The improved mass transfer and increased reaction sites work synergistically to optimize the conversion process, making the reaction more efficient and potentially reducing the time required to achieve desired conversion levels.

Increasing catalyst dosage has been consistently shown to enhance the conversion of FFAs to esters across various studies. This trend is particularly evident in biodiesel production, where higher catalyst concentrations often lead to improved conversion rates and product quality. The study utilizing Cr-Ti mixed oxides catalyst demonstrated that a 2.0 wt.% dosage resulted in FAME density closely matching that of standard palm oil biodiesel [59]. This finding suggests that optimizing catalyst dosage can significantly impact the final product's properties, potentially improving its compatibility with existing biodiesel standards. Further supporting this trend, research employing SnPMo catalyst revealed that catalyst dosage affected FFA conversion [60]. Buasri et al. [61] also reported that the increase in catalysts dosage from 2–4 wt.% increased the FFA conversion.

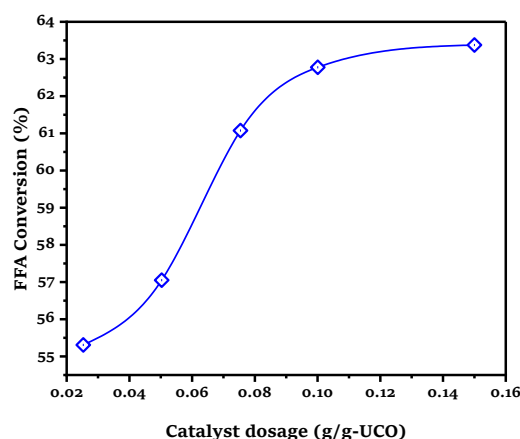


Figure 7 The effect of catalyst dosage on FFA conversion.

The relationship between catalyst dosage and conversion rate appears to be positively correlated, although it is important to note that there may be an upper limit beyond which further increases in catalyst concentration yield diminishing returns or potentially adverse effects. As shown in Figure 7, the increase in catalyst dosage after 0.1 g/g-UCO doesn't increase the conversion significantly. It's only increased by 0.6% (from 62.78% to 63.38%). It indicates that further increase in catalyst dosage doesn't improve the FFA conversion. The observed phenomenon is likely attributable to the high availability of active sites, coupled with an insufficient quantity of reactants, which consequently led to a reduction in FFA conversion. Furthermore, the negligible increase in FFA conversion can also be attributed to mass transfer limitations at elevated catalyst loadings. This result is in accordance with Roslan et al. [37]. They reported that at high catalysts dosage, it only helped to improve the reaction rate, but the final conversion remains the same.

### 3.2.4. The effect of reaction temperature

Temperature plays a pivotal role in esterification reactions, influencing multiple aspects of the process. As noted by Wan Kamis et al. [62], the reaction rate, conversion efficiency, and formation of by-products are all significantly impacted by temperature variations. Higher temperatures typically accelerate the reaction kinetics, leading to increased conversion rates. However, this acceleration comes with potential drawbacks, as elevated temperatures can also promote undesirable side reactions and by-product formation, as highlighted by Maquirriain et al. [63]. In addition, the optimal temperature for esterification reactions is not universal and depends on various factors, including the specific catalyst employed and the characteristics of the feedstock. For instance, in the context of UCO esterification, the optimal temperature may differ from that of other feedstocks due to variations in fatty acid composition and impurity content. Consequently, a thorough investigation of temperature effects in UCO esterification is crucial for process optimization. Figure 8 depicts the effect of temperature on FFA conversion.

As can be observed in Figure 8, the FFA conversion increases from 53.84% to 66.49% with the increase in reaction temperature from 40 °C to 65 °C. This demonstrates the complex interplay between thermal energy and reaction dynamics. As temperature rises, the viscosity of the reaction mixture decreases, enhancing the mobility of reactant molecules. This improved mobility leads to more frequent and effective collisions between reactants, thereby accelerating the reaction rate. The enhanced miscibility at higher temperatures also contributes to a more homogeneous reaction environment, allowing for better contact between the FFA molecules and the catalyst or other reactants. This phenomenon aligns with the Arrhenius equation, which describes the temperature dependence of reaction rates. In

agreement with the literatures [54,64], the temperature notably increased the reaction rate and the equilibrium constant, while simultaneously enhancing the mass transfer limitation.

The influence of temperature on the conversion of FFA in waste frying oil and oleic acid esterification has been extensively studied. Buasri et al. [61] demonstrated a significant increase in FFA conversion as temperatures rose from 50 °C to 80 °C in waste frying oil. This finding aligns with Wan et al. [65], who observed enhanced conversion rates in oleic acid esterification using a chromium-tungsten mixed oxide catalyst at elevated temperatures. These results underscore the critical role of temperature in promoting reaction kinetics and improving overall conversion efficiencies. Further supporting this trend, Ayan et al. [66] and Su et al. [67] emphasized that higher temperatures contribute to accelerated reaction rates and increased conversion efficiencies. This phenomenon can be attributed to the enhanced molecular kinetic energy at elevated temperatures, which facilitates more frequent and effective collisions between reactant molecules. Consequently, the activation energy barrier is more readily overcome, leading to faster reaction rates and higher product yields.

Figure 8 illustrates that the optimum temperature for achieving the FFA conversion is around 60 °C, yielding a conversion rate of 65.75%. Beyond this temperature, increasing to 65 °C does not result in a significant improvement in FFA conversion efficiency (FFA conversion of 66.49%). This plateau effect suggests that the reaction reaches a thermal threshold where further temperature elevation offers diminishing returns in catalytic activity or reaction kinetics. The limited increase in FFA conversion at temperatures above 60 °C can be attributed primarily to methanol losses due to vaporization [68,69]. As the temperature rises, methanol, which acts as a reactant in the conversion process, tends to evaporate more rapidly, reducing its effective concentration in the reaction mixture.

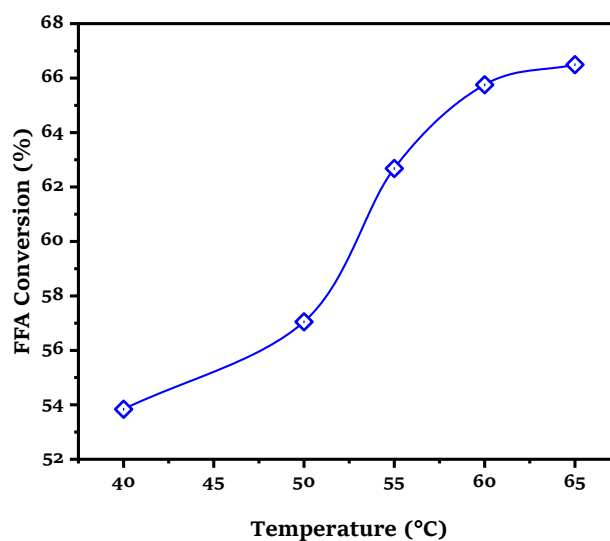


Figure 8 The effect of temperature on FFA conversion.

This loss of methanol limits the availability of the reactant needed for continuous conversion, thereby counteracting any potential gains from higher temperatures. Consequently, maintaining the temperature at 60 °C optimizes the balance between reaction rate and methanol retention, ensuring maximum conversion efficiency.

### 3.2.5. Reusability of catalyst

The reusability study of the catalyst was performed under controlled conditions, specifically using a catalyst dosage of 0.05 g/g-UCO, at a temperature of 55 °C, and with a methanol to UCO molar ratio of 10. Before initiating the reusability tests, the spent catalysts underwent a regeneration process to restore their activity and remove any contaminants accumulated during the reaction. The regeneration procedure involved washing the spent catalysts with n-hexane, which effectively removed residual oils and impurities adhering to the catalyst surface. Following this cleaning step, the catalysts were subjected to calcination at 500 °C for 3 h. This high-temperature treatment served to decompose any remaining organic residues and to re-establish the catalyst's active sites by restoring its surface properties. After calcination, the catalysts were cooled and then reused in the reusability testing to assess their stability and catalytic efficiency across successive reaction cycles.

Figure 9(a) illustrates the reusability performance of the ZSM-5 catalyst in the esterification of UCO. The data indicate that the catalyst maintains considerable stability over multiple reaction cycles. Specifically, the FFA conversion rate shows only a slight decline, decreasing from 62.68% in the initial cycle to 58.23% after five consecutive cycles. This modest reduction suggests that the catalyst retains most of its activity, highlighting its potential for repeated use without significant loss of efficiency. The observed stability of the ZSM-5 catalyst is an important factor for its practical application in a low-cost biodiesel production, as it implies reduced costs and resource consumption associated with catalyst replacement. The minor decrease in conversion efficiency could be attributed to factors such as catalyst fouling, slight structural changes, or active site blockage during the reaction cycles. Nonetheless, the catalyst's ability to sustain a high conversion rate over multiple cycles demonstrates its robustness and suitability for sustainable esterification processes involving UCO feedstock.

Figure 9(b) and Figure 9(c) present the IR spectra of UCO before and after esterification, respectively. The spectra are shown at wavenumbers around 1900–1600  $\text{cm}^{-1}$ , corresponding to the carbonyl (C=O) structure of organic compounds.

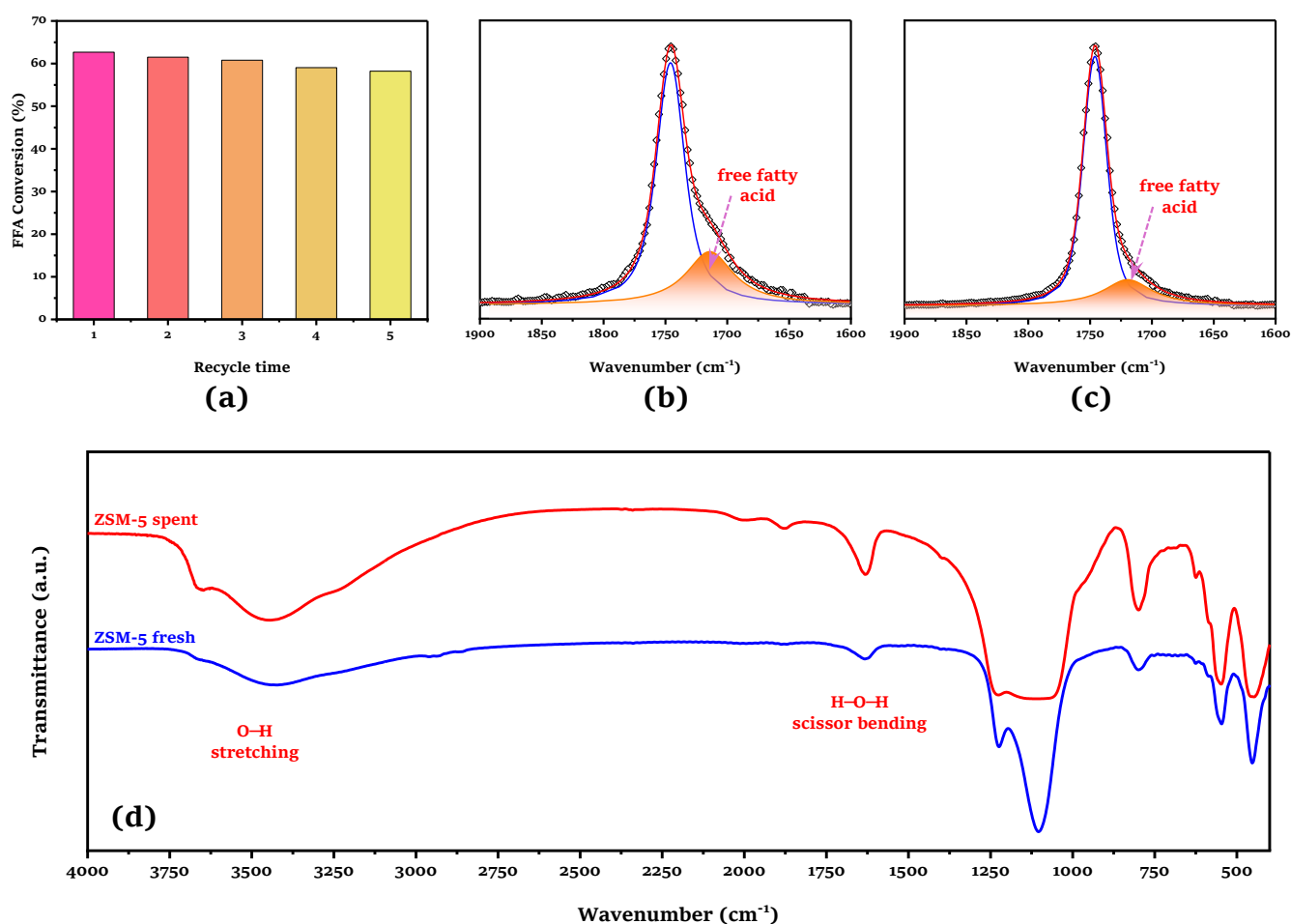


**Figure 9** Reusability of ZSM-5 catalyst in UCO esterification using catalyst dosage of 0.05 g/g-UCO, temperature of 55 °C and methanol to UCO ratio of 10 for 1 h (a); IR spectra of UCO before esterification (b); IR spectra of UCO after esterification (c); and IR spectra of fresh and spent ZSM5 catalysts (d).

Notably, two distinct peaks appear at  $1745\text{ cm}^{-1}$  and  $1715\text{ cm}^{-1}$ , attributed to the stretching vibrations of the carbonyl group from the ester structure and the carboxylic acid structure, respectively [20]. The ester structure corresponds to the triglyceride structure of UCO and the carboxylic acid structure corresponds to the FFA component. Following the esterification reaction, the peak at  $1715\text{ cm}^{-1}$  diminishes, indicating a reduction in the fatty acid components in UCO.

Figure 9(d) shows the IR spectra of the fresh ZSM-5 catalyst and the spent ZSM-5 catalyst after undergoing five consecutive reaction cycles. As can be seen, no significant changes can be observed between the two spectra, suggesting that the catalyst's structural integrity and active sites remain largely intact throughout the repeated use. This stability in the IR spectral features implies that the catalyst does not undergo significant chemical or physical degradation during the reaction and regeneration processes. Consequently, the ZSM-5 catalyst demonstrates excellent recyclability and durability, making it a reliable choice for sustained catalytic applications.

#### 4. Limitations

This study focused on ZSM-5 with MFI structure and HY with Faujasite structure. It provides valuable insights into the esterification process of used cooking oil (UCO) using specific zeolite catalysts. However, this narrow scope limits the comprehensive understanding of zeolite-catalyzed esterification. To gain a more complete picture, it is crucial to investigate a broader range of zeolite types with diverse structural characteristics. Expanding the research to include other zeolite frameworks could reveal important structure-activity relationships in UCO esterification. These different zeolite structures vary in pore size, channel systems, and acid site distribution, which may significantly influence catalytic performance, selectivity, and stability. Additionally, studying a wider array of zeolites could provide insights into the underlying mechanisms of the esterification reaction and how zeolite structure impacts the conversion of different fatty acid components present in UCO.

#### 5. Conclusions

This study demonstrates the potential of zeolite-based catalysts, particularly ZSM-5, for the esterification of used cooking oil to produce biodiesel feedstock. The superior performance of ZSM-5 compared to HY zeolite can be attributed to its higher acid density, stronger Brønsted acidity, and optimal pore structure. XRD analysis revealed distinct crystal structures for the catalysts, with ZSM-5 exhibiting an orthorhombic MFI structure and HY displaying a cubic Faujasite structure.  $\text{N}_2$  physisorption analysis showed the presence of micropores and narrow mesopores in the catalysts, with HY exhibiting a peak at 2.5–5 nm pore sizes and a shoulder at 5–10 nm.  $\text{NH}_3$ -TPD analysis indicated that

all catalysts possess weak, moderate, and strong acid sites, with ZSM-5 having a higher acid density compared to HY. In addition, based on pyridine-probed FT-IR analysis, ZSM-5 catalyst has a higher Brønsted acid site. The systematic investigation of reaction parameters revealed that increasing methanol-to-oil ratio, catalyst dosage, and temperature generally improved FFA conversion, with optimal conditions identified. ZSM-5 demonstrated superior performance with a 61.07% FFA conversion rate, while HY achieved a slightly lower conversion rate of 57.64%. The highest FFA conversion, reaching 68.30%, was achieved using a ZSM-5 catalyst at a temperature of  $50\text{ }^\circ\text{C}$ , with a catalyst dosage of  $0.05\text{ g/g-UCO}$  and a methanol-to-oil ratio of 20, over a 60-min reaction period. Under these conditions, the final AV was  $2.68\text{ mg KOH/g}$ . Although this lowest AV remains relatively high for subsequent base-catalyzed transesterification processes, the study underscores the potential of zeolite-based catalysts in the sustainable production of biodiesel from low-grade feedstocks, thereby contributing to the development of cost-effective and environmentally friendly processes.

#### Supplementary materials

No supplementary materials are available.

#### Data availability statement

The data that support the findings of this study are available from the corresponding author upon reasonable request.

#### Acknowledgments

None.

#### Author contributions

Conceptualization: T.R.  
Data curation: T.R.  
Formal Analysis: T.R., H.D.A., A.P.S.  
Funding acquisition: T.R.  
Investigation: T.R., H.D.A., A.P.S.  
Methodology: T.R., H.D.A.  
Project administration: T.R.  
Resources: T.R.  
Software: T.R.  
Supervision: T.R., H.D.A., A.P.S.  
Validation: T.R., H.D.A., A.P.S.  
Visualization: T.R.  
Writing – original draft: T.R.  
Writing – review & editing: T.R., H.D.A., A.P.S.

#### Conflict of interest

The authors declare no conflict of interest.

#### Additional information

Authors IDs:

T. Riyanto, Scopus ID [57208816811](https://orcid.org/0000-0001-5720-8816);  
H.D. Ariyanto, Scopus ID [57194876282](https://orcid.org/0000-0001-5719-4876);  
A.P. Siswanto, Scopus ID [57211134256](https://orcid.org/0000-0001-5721-1134).

Websites:

Universitas Diponegoro: <https://www.undip.ac.id/>.  
Industrial Chemical Engineering Technology: <https://trki.vokasi.undip.ac.id/>

## References

- Tabatabaei M, Karimi K, Sárvári Horváth I, Kumar R. Recent trends in biodiesel production. *Biofuel Res J*. 2015;2(3):258-267. doi:[10.18331/BRJ2015.2.3.4](https://doi.org/10.18331/BRJ2015.2.3.4)
- Kawentar WA, Budiman A. Synthesis of Biodiesel from Second-Used Cooking Oil. *Energy Procedia*. 2013;32:190-199. doi:[10.1016/j.egypro.2013.05.025](https://doi.org/10.1016/j.egypro.2013.05.025)
- Hidayat A, Rochmadi, Wijaya K, Budiman A. Esterification of Free Fatty Acid on Palm Fatty Acid Distillate using Activated Carbon Catalysts Generated from Coconut Shell. *Procedia Chem*. 2015;16:365-371. doi:[10.1016/j.proche.2015.12.065](https://doi.org/10.1016/j.proche.2015.12.065)
- Sharma YC, Singh B. Development of biodiesel: Current scenario. *Renew Sustain Energy Rev*. 2009;13(6-7):1646-1651. doi:[10.1016/j.rser.2008.08.009](https://doi.org/10.1016/j.rser.2008.08.009)
- Leung DYC, Wu X, Leung MKH. A review on biodiesel production using catalyzed transesterification. *Appl Energy*. 2010;87(4):1083-1095. doi:[10.1016/j.apenergy.2009.10.006](https://doi.org/10.1016/j.apenergy.2009.10.006)
- Marchetti JM, Miguel VU, Errazu AF. Heterogeneous esterification of oil with high amount of free fatty acids. *Fuel*. 2007;86(5-6):906-910. doi:[10.1016/j.fuel.2006.09.006](https://doi.org/10.1016/j.fuel.2006.09.006)
- Issariyakul T, Dalai AK. Biodiesel from vegetable oils. *Renew Sustain Energy Rev*. 2014;31:446-471. doi:[10.1016/j.rser.2013.11.001](https://doi.org/10.1016/j.rser.2013.11.001)
- Mandari V, Devarai SK. Biodiesel Production Using Homogeneous, Heterogeneous, and Enzyme Catalysts via Transesterification and Esterification Reactions: a Critical Review. *Bio-Energy Res*. 2022;15(2):935-961. doi:[10.1007/s12155-021-10333-w](https://doi.org/10.1007/s12155-021-10333-w)
- Thawornprasert J, Somnuk K. Two-Step Esterification Process of Palm Fatty Acid Distillate Using Soaking Coupled with Ultrasound: Process Optimization and Reusable Solid Acid Catalysts. *ACS Omega*. 2024;9(51):50427-50438. doi:[10.1021/acsomega.4c07449](https://doi.org/10.1021/acsomega.4c07449)
- Wang L, Dong X, Jiang H, Li G, Zhang M. Ordered mesoporous carbon supported ferric sulfate: A novel catalyst for the esterification of free fatty acids in waste cooking oil. *Fuel Process Technol*. 2014;128:10-16. doi:[10.1016/j.fuproc.2014.06.023](https://doi.org/10.1016/j.fuproc.2014.06.023)
- Kawashima A, Matsubara K, Honda K. Acceleration of catalytic activity of calcium oxide for biodiesel production. *Bioreour Technol*. 2009;100(2):696-700. doi:[10.1016/j.biortech.2008.06.049](https://doi.org/10.1016/j.biortech.2008.06.049)
- Gaurav A, Dumas S, Mai CTQ, Ng FTT. A kinetic model for a single step biodiesel production from a high free fatty acid (FFA) biodiesel feedstock over a solid heteropolyacid catalyst. *Green Energy Environ*. 2019;4(3):328-341. doi:[10.1016/j.gee.2019.03.004](https://doi.org/10.1016/j.gee.2019.03.004)
- Ketzer F, Celante D, de Castilhos F. Catalytic performance and ultrasonic-assisted impregnation effects on WO<sub>3</sub>/USY zeolites in esterification of oleic acid with methyl acetate. *Microporous Mesoporous Mater*. 2020;291:109704. doi:[10.1016/j.micromeso.2019.109704](https://doi.org/10.1016/j.micromeso.2019.109704)
- Prates CD, Ballotin FA, Limborço H, Ardisson JD, Lago RM, Teixeira AP de C. Heterogeneous acid catalyst based on sulfated iron ore tailings for oleic acid esterification. *Appl Catal A Gen*. 2020;600:117624. doi:[10.1016/j.apcata.2020.117624](https://doi.org/10.1016/j.apcata.2020.117624)
- Cadenas M, Bringué R, Fité C, Iborra M, Ramírez E, Cunill F. Alkylation of toluene with 1-hexene over macroreticular ion-exchange resins. *Appl Catal A Gen*. 2014;485:143-148. doi:[10.1016/j.apcata.2014.07.044](https://doi.org/10.1016/j.apcata.2014.07.044)
- Osazuwa OU, Abidin SZ. The Functionality of Ion Exchange Resins for Esterification, Transesterification and Hydrogenation Reactions. *ChemistrySelect*. 2020;5(25):7658-7670. doi:[10.1002/slct.202001381](https://doi.org/10.1002/slct.202001381)
- Yusuf BO, Oladepo SA, Ganiyu SA. Biodiesel Production from Waste Cooking Oil via  $\beta$ -Zeolite-Supported Sulfated Metal Oxide Catalyst Systems. *ACS Omega*. 2023;8(26):23720-23732. doi:[10.1021/acsomega.3c01892](https://doi.org/10.1021/acsomega.3c01892)
- Mateos PS, Ruscitti CB, Casella ML, Matkovic SR, Briand LE. Phosphotungstic Wells-Dawson Heteropolyacid as Potential Catalyst in the Transesterification of Waste Cooking Oil. *Catalysts*. 2023;13(9):1253. doi:[10.3390/catal13091253](https://doi.org/10.3390/catal13091253)
- Istadi I, Kusumawati Y, Riyanto T, Anggoro DD, Jongsomjit B, Putranto AB. Enhancing spent RFCC catalysts for biofuel production: Ultrasound-assisted acid treatment for improved crystallinity, pore size, and acid site ratio. *Case Stud Chem Environ Eng*. 2024;10:100843. doi:[10.1016/j.cscee.2024.100843](https://doi.org/10.1016/j.cscee.2024.100843)
- Istadi I, Riyanto T, Anggoro DD, Pramana CS, Ramadhani AR. High Acidity and Low Carbon-Coke Formation Affinity of Co-Ni/ZSM-5 Catalyst for Renewable Liquid Fuels Production through Simultaneous Cracking-Deoxygenation of Palm Oil. *Bull Chem React Eng Catal*. 2023;18(2):222-237. doi:[10.9767/bcrec.17974](https://doi.org/10.9767/bcrec.17974)
- Chung KH, Chang DR, Park BG. Removal of free fatty acid in waste frying oil by esterification with methanol on zeolite catalysts. *Bioresour Technol*. 2008;99(16):7438-7443. doi:[10.1016/j.biortech.2008.02.031](https://doi.org/10.1016/j.biortech.2008.02.031)
- Hayyan A, Alam MZ, Mirghani MES, Kabbashi NA, Hakimi NINM, Siran YM, Tahiruddin S. Sludge palm oil as a renewable raw material for biodiesel production by two-step processes. *Bioresour Technol*. 2010;101(20):7804-7811. doi:[10.1016/j.biortech.2010.05.045](https://doi.org/10.1016/j.biortech.2010.05.045)
- Tarigan JB, Barus AF, Simamora NT, Tarigan RS, Perangin-angin S, Ginting J, Sitepu EK, Taufiq-Yap YH. Microwave-intensified esterification of high-free fatty acid feedstock into biodiesel using waste chicken eggshells as a heterogeneous catalyst. *Case Stud Chem Environ Eng*. 2025;11:101107. doi:[10.1016/j.cscee.2025.101107](https://doi.org/10.1016/j.cscee.2025.101107)
- Luz PTS da, Moraes BF de, Ferreira RK, Melo CC de, Oliveira A de N de, Costa AAF da, Costa CEF da, Rocha Filho GN da, Osman SM, Luque R, Nascimento LAS do. Design of activated bentonite-based catalysts for the esterification of residual free fatty acids from palm oil. *Catal Today*. 2024;441:114886. doi:[10.1016/j.cattod.2024.114886](https://doi.org/10.1016/j.cattod.2024.114886)
- Oliveira AA, Santos RPS, Rocha WS, de Luna FMT, Fernandez-Lafuente R, Monteiro RRC, Vieira RS. Design of a biolubricant by the enzymatic esterification of the free fatty acids from castor oil with neopentylglycol. *Process Biochem*. 2024;147:318-331. doi:[10.1016/j.procbio.2024.09.007](https://doi.org/10.1016/j.procbio.2024.09.007)
- Zhang J, Li X, Liu J, Wang C. A Comparative Study of MFI Zeolite Derived from Different Silica Sources: Synthesis, Characterization and Catalytic Performance. *Catalysts*. 2018;9(1):13. doi:[10.3390/catal9010013](https://doi.org/10.3390/catal9010013)
- Riyanto T, Istadi I, Jongsomjit B, Anggoro DD, Pratama AA, Faris MA Al. Improved Brønsted to Lewis (B/L) Ratio of Co and Mo-Impregnated ZSM-5 Catalysts for Palm Oil Conversion to Hydrocarbon-Rich Biofuels. *Catalysts*. 2021;11(11):1286. doi:[10.3390/catal11111286](https://doi.org/10.3390/catal11111286)
- Reinoso D, Adrover M, Pedernera M. Green synthesis of nanocrystalline faujasite zeolite. *Ultrason Sonochem*. 2018;42:303-309. doi:[10.1016/j.ultsonch.2017.11.034](https://doi.org/10.1016/j.ultsonch.2017.11.034)
- Aloulou H, Bouhamed H, Ghorbel A, Amar R Ben, Khemakhem S. Elaboration and characterization of ceramic microfiltration membranes from natural zeolite: application to the treatment of cuttlefish effluents. *Desalin Water Treat*. 2017;95:9-17. doi:[10.5004/dwt.2017.21348](https://doi.org/10.5004/dwt.2017.21348)
- Mohamed MM, Zidan FI, Thabet M. Synthesis of ZSM-5 zeolite from rice husk ash: Characterization and implications for photocatalytic degradation catalysts. *Microporous Mesoporous Mater*. 2008;108(1-3):193-203. doi:[10.1016/j.micromeso.2007.03.043](https://doi.org/10.1016/j.micromeso.2007.03.043)
- Chung NH, Dien LQ, Cuong TD, Van Lieu N, Hoang PH. Influence of the acidity of solid catalyst HSO<sub>3</sub>-ZSM-5 on the hydrolysis of pretreated corncob. *RSC Adv*. 2018;8(73):41776-41781. doi:[10.1039/C8RA09190K](https://doi.org/10.1039/C8RA09190K)
- Thommes M, Kaneko K, Neimark AV, Olivier JP, Rodriguez-Reinoso F, Rouquerol J, Sing KSW. Physisorption of gases, with special reference to the evaluation of surface area and pore size distribution (IUPAC Technical Report). *Pure Appl Chem*. 2015;87(9-10):1051-1069. doi:[10.1515/pac-2014-1117](https://doi.org/10.1515/pac-2014-1117)

33. Sing KSW, Williams RT. Physisorption Hysteresis Loops and the Characterization of Nanoporous Materials. *Adsorpt Sci Technol*. 2004;22(10):773-782. doi:[10.1260/0263617053499032](https://doi.org/10.1260/0263617053499032)
34. Klaewkla R, Arend M, F. W. A Review of Mass Transfer Controlling the Reaction Rate in Heterogeneous Catalytic Systems. In: *Mass Transfer - Advanced Aspects*. InTech; 2011. doi:[10.5772/22962](https://doi.org/10.5772/22962)
35. Singh L, Rekha P, Chand S. Cu-impregnated zeolite Y as highly active and stable heterogeneous Fenton-like catalyst for degradation of Congo red dye. *Sep Purif Technol*. 2016;170:321-336. doi:[10.1016/j.seppur.2016.06.059](https://doi.org/10.1016/j.seppur.2016.06.059)
36. Gu Y, Cui N, Yu Q, Li C, Cui Q. Study on the influence of channel structure properties in the dehydration of glycerol to acrolein over H-zeolite catalysts. *Appl Catal A Gen*. 2012;429-430:9-16. doi:[10.1016/j.apcata.2012.03.030](https://doi.org/10.1016/j.apcata.2012.03.030)
37. Roslan NA, Zainal Abidin S, Abdullah N, Osazuwa OU, Abdul Rasid R, Yunus NM. Esterification reaction of free fatty acid in used cooking oil using sulfonated hypercrosslinked exchange resin as catalyst. *Chem Eng Res Des*. 2022;180:414-424. doi:[10.1016/j.cherd.2021.10.020](https://doi.org/10.1016/j.cherd.2021.10.020)
38. Suprun W, Lutecki M, Haber T, Papp H. Acidic catalysts for the dehydration of glycerol: Activity and deactivation. *J Mol Catal A Chem*. 2009;309(1-2):71-78. doi:[10.1016/j.molcata.2009.04.017](https://doi.org/10.1016/j.molcata.2009.04.017)
39. Musa ML, Mat R, Tuan Abdullah TA. Catalytic Conversion of Residual Palm Oil in Spent Bleaching Earth (SBE) By HZSM-5 Zeolite based-Catalysts. *Bull Chem React Eng Catal*. 2018;13(3):456-465. doi:[10.9767/bcrec.13.3.1929.456-465](https://doi.org/10.9767/bcrec.13.3.1929.456-465)
40. Chen C, Zhang Q, Meng Z, Li C, Shan H. Effect of magnesium modification over H-ZSM-5 in methanol to propylene reaction. *Appl Petrochem Res*. 2015;5(4):277-284. doi:[10.1007/s13203-015-0129-7](https://doi.org/10.1007/s13203-015-0129-7)
41. Hensen EJM, Poduval DG, Degirmenci V, Ligthart D. JM, Chen W, Maugé F, Rigutto MS, Veen JAR van. Acidity Characterization of Amorphous Silica-Alumina. *J Phys Chem C*. 2012;116(40):21416-21429. doi:[10.1021/jp309182f](https://doi.org/10.1021/jp309182f)
42. Deka RC. Acidity in zeolites and their characterization by different spectroscopic methods. *Indian J Chem Technol*. 1998;5(3):109-123.
43. Bailleul S, Yarulina I, Hoffman AEJ, Dokania A, Abou-Hamad E, Chowdhury AD, Pieters G, Hajek J, De Wispelaere K, Warquier M, Gascon J, Van Speybroeck V. A Supramolecular View on the Cooperative Role of Brønsted and Lewis Acid Sites in Zeolites for Methanol Conversion. *J Am Chem Soc*. 2019;141(37):14823-14842. doi:[10.1021/jacs.9b07484](https://doi.org/10.1021/jacs.9b07484)
44. Derouane EG, Védrine JC, Pinto RR, Borges PM, Costa L, Lemos MANDA, Lemos F, Ribeiro FR. The Acidity of Zeolites: Concepts, Measurements and Relation to Catalysis: A Review on Experimental and Theoretical Methods for the Study of Zeolite Acidity. *Catal Rev*. 2013;55(4):454-515. doi:[10.1080/01614940.2013.822266](https://doi.org/10.1080/01614940.2013.822266)
45. Khder AERS, Hassan HMA, El-Shall MS. Metal-organic frameworks with high tungstophosphoric acid loading as heterogeneous acid catalysts. *Appl Catal A Gen*. 2014;487:110-118. doi:[10.1016/j.apcata.2014.09.012](https://doi.org/10.1016/j.apcata.2014.09.012)
46. Shestakova P, Popova M, Szegedi Á, Lazarova H, Nga Luong TK, Trendafilova I, Mihály J, Parac-Vogt TN. Hybrid catalyst with combined Lewis and Brønsted acidity based on ZrIV substituted polyoxometalate grafted on mesoporous MCM-41 silica for esterification of renewable levulinic acid. *Microporous Mesoporous Mater*. 2021;323:111203. doi:[10.1016/j.micromeso.2021.111203](https://doi.org/10.1016/j.micromeso.2021.111203)
47. Shu Q, Liu X, Huo Y, Tan Y, Zhang C, Zou L. Construction of a Brønsted-Lewis solid acid catalyst La-PW-SiO<sub>2</sub>/SWCNTs based on electron withdrawing effect of La(III) on  $\pi$  bond of SWCNTs for biodiesel synthesis from esterification of oleic acid and methanol. *Chinese J Chem Eng*. 2022;44:351-362. doi:[10.1016/j.cjche.2021.02.002](https://doi.org/10.1016/j.cjche.2021.02.002)
48. Munyentwali A, Li H, Yang Q. Review of advances in bifunctional solid acid/base catalysts for sustainable biodiesel production. *Appl Catal A Gen*. 2022;633:118525. doi:[10.1016/j.apcata.2022.118525](https://doi.org/10.1016/j.apcata.2022.118525)
49. Koo HM, Lee JH, Chang TS, Suh YW, Lee DH, Bae JW. Esterification of acetic acid with methanol to methyl acetate on Pd-modified zeolites: effect of Brønsted acid site strength on activity. *React Kinet Mech Catal*. 2014;112(2):499-510. doi:[10.1007/s11144-014-0713-3](https://doi.org/10.1007/s11144-014-0713-3)
50. Chen F, Kim S, Barpaga D, Fulton JL, Motkuri RK, Gutiérrez OY, Camaioni DM, Lercher JA. Activity of Brønsted Acid Sites in UiO-66 for Cyclohexanol Dehydration. *Top Catal*. 2023;66(15-16):1196-1201. doi:[10.1007/s11244-023-01830-7](https://doi.org/10.1007/s11244-023-01830-7)
51. Wang K, Zhang X, Zhang J, Zhang Z, Fan C, Han P. Theoretical Study on Free Fatty Acid Elimination Mechanism for Waste Cooking Oils to Biodiesel over Acid Catalyst. *J Mol Graph Model*. 2016;66:41-46. doi:[10.1016/j.jmglm.2016.03.002](https://doi.org/10.1016/j.jmglm.2016.03.002)
52. Liu Y, Lu H, Liang B. Effect of Water on the Pre-Esterification of *Jatropha curcas* L. Oil for Biodiesel Production. *J Biobased Mater Bioenergy*. 2009;3(4):342-347. doi:[10.1166/jbmb.2009.1045](https://doi.org/10.1166/jbmb.2009.1045)
53. Dal Pozzo DM, Azevedo dos Santos JA, Júnior ES, Santos RF, Feiden A, Melegari de Souza SN, Burgardt I. Free fatty acids esterification catalyzed by acid Faujasite type zeolite. *RSC Adv*. 2019;9(9):4900-4907. doi:[10.1039/C8RA10248A](https://doi.org/10.1039/C8RA10248A)
54. Ong HR, Khan MR, Chowdhury MNK, Yousuf A, Cheng CK. Synthesis and characterization of CuO/C catalyst for the esterification of free fatty acid in rubber seed oil. *Fuel*. 2014;120:195-201. doi:[10.1016/j.fuel.2013.12.015](https://doi.org/10.1016/j.fuel.2013.12.015)
55. Ramadhas A, Jayaraj S, Muraleedharan C. Biodiesel production from high FFA rubber seed oil. *Fuel*. 2005;84(4):335-340. doi:[10.1016/j.fuel.2004.09.016](https://doi.org/10.1016/j.fuel.2004.09.016)
56. Xie W, Qi C, Wang H, Liu Y. Phenylsulfonic acid functionalized mesoporous SBA-15 silica: A heterogeneous catalyst for removal of free fatty acids in vegetable oil. *Fuel Process Technol*. 2014;119:98-104. doi:[10.1016/j.fuproc.2013.10.028](https://doi.org/10.1016/j.fuproc.2013.10.028)
57. Gan S, Ng HK, Chan PH, Leong FL. Heterogeneous free fatty acids esterification in waste cooking oil using ion-exchange resins. *Fuel Process Technol*. 2012;102:67-72. doi:[10.1016/j.fuproc.2012.04.038](https://doi.org/10.1016/j.fuproc.2012.04.038)
58. Yunus NM, Zainal Abidin S, Sim Yee C. Studies on the performance of tubular flow reactor for esterification of free fatty acid from used cooking oil using highly porous cation exchange resin as catalyst. *Energy Sources, Part A Recover Util Environ Eff*. 2018;40(21):2518-2527. doi:[10.1080/15567036.2018.1503757](https://doi.org/10.1080/15567036.2018.1503757)
59. Roslan MF, Wan Z, Halim SF, Isa N, Bashah NAA. Effects of catalyst dosage and reaction time in the esterification of PFAD to produce FAME. *AIP Conf Proc*. 2023;3013:050024. doi:[10.1063/5.0148610](https://doi.org/10.1063/5.0148610)
60. Lai J, Wang J, Luo G, Liu C. Synthesis of Fatty Acid Esters by Esterification of Oleic Acid and Methanol Over Phosphomolybdenum Heteropolyacid. *Pet Process Petrochemicals*. 2012;43(12):14-18.
61. Buasri A, Chaiyut N, Loryuenyong V, Pin-Ngern K, Tonprasert N, Dangnuan S. Production of Fatty Acid Methyl Ester by Esterification of Waste Frying Oil with Methanol Using Acidified Silica as Heterogeneous Catalyst. *J Biobased Mater Bioenergy*. 2013;7(2):229-232. doi:[10.1166/jbmb.2013.1332](https://doi.org/10.1166/jbmb.2013.1332)
62. Wan Kamis WZ, Azuwar WN, Ali Bashah NA, Isa N, Syed-Hasan SSA. Effect of reaction conditions in the catalytic esterification of palm fatty acid distillate to produce fatty acid methyl ester. *J Phys Conf Ser*. 2019;1349(1):012116. doi:[10.1088/1742-6596/1349/1/012116](https://doi.org/10.1088/1742-6596/1349/1/012116)
63. Maquirriain MA, Querini CA, Pisarello ML. Glycerine esterification with free fatty acids: Homogeneous catalysis. *Chem Eng Res Des*. 2021;171:86-99. doi:[10.1016/j.cherd.2021.04.018](https://doi.org/10.1016/j.cherd.2021.04.018)
64. Al-Sakkari EG, Abdeldayem OM, El-Sheltawy ST, Abadir MF, Soliman A, Rene ER, Ismail I. Esterification of high FFA content waste cooking oil through different techniques including

- the utilization of cement kiln dust as a heterogeneous catalyst: A comparative study. *Fuel*. 2020;279:118519. doi:[10.1016/j.fuel.2020.118519](https://doi.org/10.1016/j.fuel.2020.118519)
65. Wan Z, Lim JK, Hameed BH. Chromium–tungsten heterogeneous catalyst for esterification of palm fatty acid distillate to fatty acid methyl ester. *J Taiwan Inst Chem Eng*. 2015;54:64-70. doi:[10.1016/j.jtice.2015.03.020](https://doi.org/10.1016/j.jtice.2015.03.020)
66. Ayan ED, Sert E, Atalay FS. An Investigation of the Production and Lubricity Characteristics of Fatty Acid Esters. *Energy Sources, Part A Recover Util Environ Eff*. 2014;36(1):64-72. doi:[10.1080/15567036.2010.551270](https://doi.org/10.1080/15567036.2010.551270)
67. Su C, Fu C, Gomes J, Chu I, Wu W. A heterogeneous acid-catalyzed process for biodiesel production from enzyme hydrolyzed fatty acids. *AIChE J*. 2008;54(1):327-336. doi:[10.1002/aic.11377](https://doi.org/10.1002/aic.11377)
68. Nayak SN, Nayak MG, Bhasin DCP. Parametric, kinetic, and thermodynamic studies of microwave-assisted esterification of Kusum oil. *Fuel Commun*. 2021;8:100018. doi:[10.1016/j.jfueco.2021.100018](https://doi.org/10.1016/j.jfueco.2021.100018)
69. Chuah LF, Bokhari A, Yusup S, Klemeš JJ, Abdullah B, Akbar MM. Optimisation and Kinetic Studies of Acid Esterification of High Free Fatty Acid Rubber Seed Oil. *Arab J Sci Eng*. 2016;41(7):2515-2526. doi:[10.1007/s13369-015-2014-1](https://doi.org/10.1007/s13369-015-2014-1)